

CONTRIBUTION OF TEMPERATURE MODULATED DSC[®] TO THE STUDY OF THE MOLECULAR MOBILITY IN GLASS FORMING PHARMACEUTICAL SYSTEMS

L. Carpentier^{}, L. Bourgeois and M. Descamps^{*}*

Laboratoire de Dynamique et Structure des Matériaux Moléculaire – U.P.R.E.S.A. CNRS 8024 – Bât. P5 - Ust Lille - 59655 Villeneuve d'Ascq, France

Abstract

The temperature modulated differential scanning calorimetry (MDSC[®]) technique has been used to characterise the low frequency molecular mobility of indomethacin and maltitol just above their respective calorimetric glass transition temperature T_g . Analysis has been made using the concept of complex specific heat. Spectroscopic information are thus obtained through the temperature dependence of the isochronal real and imaginary parts C' and C'' . This gives access to the fragility index m and the stretched exponent β . The comparison with dielectric spectroscopy has been performed to check the coherence of spectroscopic information. Measurements on maltitol enable to demonstrate the useful complementarity of the technique when the low frequencies dielectric relaxations are occulted by the presence of conductors default.

Keywords: dielectric relaxation, glass transition, molecular mobility, pharmaceutical, relaxation time, specific heat spectroscopy

Introduction

The molecular mobility is a fundamental feature of the physical state of active substances and excipients. Its characterisation is determinant for the control and the prediction of their bioavailability with regard to the stability and solubility of materials. This concerns particularly the amorphous and glassy states. Many molecular processes, such as those that occur during crystallisation and chemical reactions in supercooled liquids and glasses, depend on the degree of mobility of the molecular species involved. The importance of the characterisation of these slow relaxation processes in pharmaceutical and food sciences has been stressed in numerous papers [1–3]. It has been shown recently [4] that Modulated DSC[®] (MDSC[®]) gives the possibility to perform specific heat spectroscopy analysis over one decade of frequency in the range 0.01 Hz–0.1 Hz which allows to investigate the dynamics of glass-forming liquids. The object of this paper is to study the applicability of modulated differential

^{*} Authors for correspondence: Fax: 00 33 3 20434084; E-mail: Marc.Descamps@univ-lille1.fr; E-mail: Laurent.Carpentier@univ-lille1.fr

scanning calorimetry to the investigation of molecular mobility of two model pharmaceutical compounds: indomethacin and maltitol. We emphasise in particular on the capacity of MDSC to determine the activation energy, the fragility and non-exponential parameter of glass forming systems. MDSC spectroscopy which is concerned with the determination of a complex heat capacity, exhibits some similarities with dielectric spectroscopy. A comparison of these two techniques is performed on the two investigated pharmaceuticals to test the MDSC data coherence and the complementarity of these two spectroscopies.

Principles of a specific heat spectroscopy analysis with MDSC

The MDSC technique has been described in several papers [5, 6]. The various ways to analyse the signals and the information they provide are described in some details [4, 7–9]. We focus here on the capability of MDSC to perform a spectroscopy of the enthalpic relaxation. Since MDSC offers one decade of frequency in the range 0.01–0.1 Hz, we thus consider only the vicinity of the thermodynamic glass transition of the compounds. Furthermore, performing the measurements upon cooling allows to avoid possible spontaneous heat flows associated to kinetic effects that are, for example, cold recrystallization or the rapid enthalpic recovery observed upon heating an annealed glass.

Signals

MDSC is a scanning technique in which a small sinusoidal temperature change T_{sm} (pulsation ω) is added to the conventional DSC temperature ramp $\bar{T}(t)$ (linear rate q). The experimentally accessible perturbations and responses are :

- The programmed temperature of the heating block [10]:

$$T(t) = \bar{T}(t) + T_{sm} = T_i + qt + A \sin \omega t \quad (1)$$

where T_i is the initial temperature of the run and A the amplitude of the temperature modulation, and the equivalent modulated heating rate:

$$\dot{T}(t) = q + \dot{T}_o \cos(\omega t) \quad (\dot{T}_o = A\omega) \quad (2)$$

- The heat flow [4] involves a linear part and an out of phase sinusoidal modulated part to which may add a heat flow contribution (\dot{Q}_{kin}) induced by possible spontaneous kinetic effects that we will not consider here:

$$\dot{Q}(t) = qC_p(q\bar{T}) + \dot{Q}_o(\bar{T}\omega)\cos(\omega t - \varphi) + (\dot{Q}_{kin}) \quad (3)$$

The first term in the relations (2) and (3) corresponds respectively to the classical DSC temperature perturbation and heat flow response, far from any kinetic event. $C_p(q\bar{T})$ is the ordinary heat capacity of the sample which, upon scanning, depends on q near a glass transition. Examples of the signals obtained on indomethacin (studied in more detail below), and recorded when scanning the glass transformation range upon

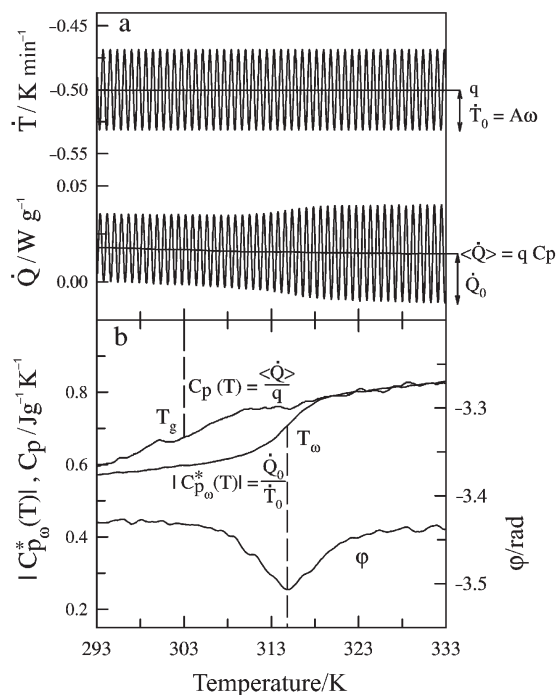


Fig 1 Temperature evolution of the main MDSC signals for indomethacin: the modulated temperature T and modulated heat flow Q ($A=0.5$ K, $\omega/2\pi=1/100$ s $^{-1}$, $q=-0.5$ K min $^{-1}$) (a). The signals which allows to determine the complex heat capacity $C_p^*(\omega)$ are calculated from T and Q (the phase lag ϕ is not corrected) (b)

cooling, are shown in Fig. 1a. The characteristic features of the approach of the glass transition shown by this measurement are (Fig. 1b for details):

- The classical jump of the average heat flow $\langle \dot{Q} \rangle$ at $T_g(q=-0.5$ K min $^{-1}$)=303 K (or equivalently the drop of $C_p(qT)$)
- The jump of the modulated heat flow amplitude \dot{Q}_0 at a temperature somewhat higher $T_\omega=314.8$ K. This jump is narrower and better resolved than that of the classical DSC signal.
- A peak in the phase lag ϕ at T_ω .

The underlying cooling rate q is responsible for the sample falling out of equilibrium at $T_g(q)$. T_ω reveals a different ergodicity breaking temperature associated to the somewhat shorter time scale of the oscillating perturbation.

Phase lag

The frequency dependence of the phase lag ϕ is shown on Fig. 2. We may notice:

- An important non-zero phase lag ϕ_{ht} over the whole temperature range which is attributed [11, 12] to heat transfers (ht) both between the sample and the thermometer

and in the sample itself. The following relation has been recently proposed [13] to rationalize this contribution:

$$\varphi_{ht} = -\omega R C_p \quad (4)$$

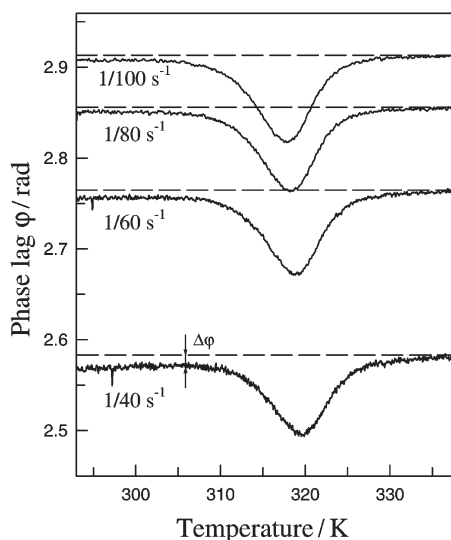


Fig. 2 Phase lag φ evolution for indomethacin as a function of temperature in the vicinity of T_g ($q = -0.1 \text{ K min}^{-1}$), at different frequencies (1/100 to 1/40 s^{-1} in steps of 1/20 s^{-1}). φ is the superposition of the phase lag φ_{ht} due to heat transfers and of the phase lag φ_0 (the phase angle peak) due to structural relaxation. From this curve no single peak in the phase lag but a superposition of a peak and a step ($\Delta\varphi$) can be observed. $\Delta\varphi$ is all the more large since the period of modulation is weak

where R is the thermal resistance of the heat flow path between the sample and the heater and C_p is the heat capacity of the sample.

- A step change $\Delta\varphi$ in the phase angle observed when passing the peak which increases with frequency. Its origin is also attributed to the heat transfers. Its amplitude can be related to the heat capacity jump ΔC_p at T_g using (4):

$$\Delta\varphi = -\omega R \Delta C_p \quad (5)$$

- A continuous shift of the phase lag peak maximum (T_ω) towards higher temperatures when the modulation frequency increases. In an other way, the peak position is not influenced by the underlying rate q .

These observations clearly reveal the relaxational origin of the phase peak. The purely relaxational part φ_0 of the phase lag can be extracted from the measured phase angle φ using:

$$\varphi_0 = \varphi - \varphi_{ht} \quad (6)$$

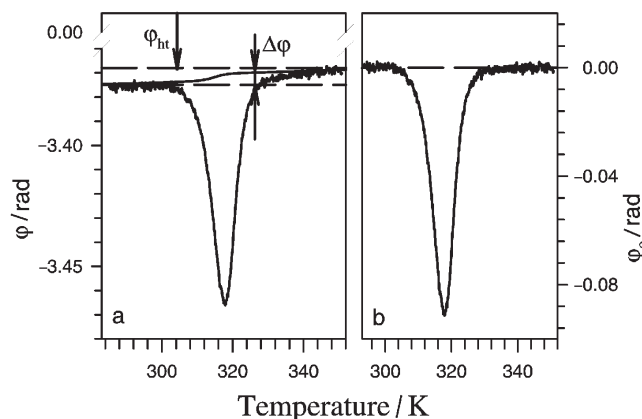


Fig. 3 Phase angle correction between heat flow rate and cooling rate of MDSC measurements of indomethacin in the glass transition region ($q = -0.1 \text{ K min}^{-1}$, $A = 0.5 \text{ K}$ and $\omega/2\pi = 1/100 \text{ s}^{-1}$). a – The total loss phase angle derived from \dot{T} and \dot{Q} . b – The corrected phase angle ϕ_0 obtained by subtracting ϕ_{ht} and $\Delta\phi$ (Eq. (6)) to ϕ

(ϕ_0 is expected to be zero far from T_g). Using (5), it has been proposed [13] to perform this correction by subtracting a curve which is proportional to the measured heat capacity and scaled in such a way that it fits to the measured phase angle outside the glass transition region. Example of this correction is shown in Fig. 3. The temperature and frequency evolution of the relaxational part ϕ_0 allows us to undertake a specific heat spectroscopy analysis with MDSC technique.

Complex heat capacity

A complex heat capacity $C_p^*(\omega)$ can be introduced to link linearly the sinusoidal modulated part of the heat flow response $\dot{Q}_{sm}(t)$ to the sinusoidal modulated part \dot{T}_{sm} of the temperature rate. In complex notation, $\dot{Q}_{sm}(t)$ can be written as follow [4, 6]:

$$\dot{Q}_{sm}(t) = \dot{Q}_0 \cos(\omega t - \phi_0) = \text{Real}(C_p^*(\omega) \dot{T}_0 e^{-i\omega t}) \quad (7)$$

where

$$C_p^*(\omega) = C' + iC'' = |C_p^*(\omega)| \exp(i\phi_0) \quad (8)$$

is the frequency dependent heat capacity. The properly corrected MDSC thermal curves give access to the module $|C_p^*(\omega)| = \dot{Q}_0 / \dot{T}_0$ and relaxational phase ϕ_0 .

The real and imaginary part of $C_p^*(\omega)$ are given by:

$$C' = \frac{\dot{Q}_0}{\dot{T}_0} \cos\phi_0; \quad C'' = \frac{\dot{Q}_0}{\dot{T}_0} \sin\phi_0 \quad (9)$$

Examples of numerical data which are necessary to obtain $C_p^*(\omega)$ in the course of a routine MDSC scan are provided by Figs 1b and 3. As was previously discussed [4],

the signal can be displaced and distorted to give an effective smearing when the two characteristic times of the technique, respectively related to the scanning rate and the modulation, are too close. This smearing effect can be largely avoided using low enough values of q (values of q lower than 0.5 K min^{-1} are recommended). The reader is referred to [14] for a comparison of specific heat spectroscopic data obtained from MDSC and the alternating current calorimetry technique [15]. It is demonstrated that the MDSC phase lag measurements give appropriate data for the shape of the susceptibility as well as their temperature evolutions.

Techniques, experimental protocols and materials

Calorimetry

A DSC 2920 TA Instruments equipped with a refrigerated cooling system (RCS) was used for the calorimetric measurements. The samples were encapsulated in aluminium crimped pans. The samples weight was in the range of 7–10 mg which is a low enough value to allow the sample to follow the imposed thermal oscillations [7]. The temperature and enthalpy were calibrated using indium as a standard. The modulus of the complex heat capacity was calibrated from the $|C_p^*(\omega)|$ measurements of sapphire in the studied temperature range. In order to minimize the heat conductivity problems, this calibration was performed at the lowest possible frequency of $1/100 \text{ s}^{-1}$. Since the measurements at the other frequencies are more affected by the conductivity, the higher frequencies calibration data were rescaled to the lower frequency data. The heat transfer contribution to the phase lag (ϕ_{ht}) was estimated according to the Weyer *et al.* suggestion [13] deduced from Eq. (4):

$$\phi_{ht} = b - k|C_p^*| \quad (10)$$

in such way that it fits to the measured phase angle on both parts of the relaxation peak – example of correction is shown in Fig. 3. Since the available frequency range is narrow ($1/20$ – $1/100 \text{ s}^{-1}$), the measurements were performed in an isochronal way. The measurements were performed upon cooling and consisted in repeated temperature scans around T_g , at various frequencies and using the same underlying linear rate $q = -0.1 \text{ K min}^{-1}$. The amplitude and frequency were chosen so that the amplitude of the modulated temperature rate is kept constant for each experiment: $\dot{T}_0 = A\omega = \pi/100$.

Dielectric measurements

Dielectric measurements were also performed in order to assess the coherency and possible complementarity of both techniques. The analyser DEA 2970 of TA Instruments was used. It provides nearly 7 decades of frequency (3 mHz–100 KHz) and allows an extended investigation at the approach of T_g ($\nu(T_g) \approx 10 \text{ mHz}$). A Liquid Nitrogen Cooling Accessory provided testing capability from 120 to 700 K and a dried airflow minimised hydration of the samples. To parallel as much as possible MDSC

measurements, the dielectric investigations were also performed in isochronal modes with the same cooling rate.

Materials

The indomethacin (1-[4-chlorobenzoyl]-5-methoxy-2-methylindole-3-acetic acid) and the maltitol (*D*-Glucitol-4-*o*- α -*D*-Glucopyranosil) were obtained from Aldrich Chemical Company Inc. Both samples were first dried under vacuum. Indomethacin was initially in the γ crystalline phase that we have checked to melt at about 435 K [16]. Upon cooling, the undercooled liquid resists against parasitic recrystallisation even at very low cooling rate. The calorimetric glass transition was observed at $T_g \approx 315$ K with a cooling rate of 5 K min^{-1} . These values agree with the published ones [17]. Upon reheating, cold crystallisation is not observed anymore. Spectroscopy measurements close to T_g could thus be performed in succession without further melting of the sample. Once melted ($T_m = 420$ K), maltitol can also be undercooled without further crystallisation and presents a glass transition at about 320 K [18].

Low frequency spectroscopy and molecular mobility of indomethacin

The real (C') and imaginary (C'') parts of the $C_p^*(\omega)$ for indomethacin are calculated by treating the data such as those of Fig. 1a–b according to Eqs (6)–(8). Figure 4a shows their temperature evolution at five different periods of modulation 100–20 s in steps of 20 s. The real part C' drops by about a factor 1.4 which is also what is observed at T_g from measurements of $C_p(q)$ alone. The temperatures of this drop however occur distinctly above $T_g(q)$ and they strongly depend on the measurement periods. The imaginary part C'' has a peak at the same temperature (T_ω) where the real part C' drops. The C' and C'' curves show the characteristic forms for the complex susceptibility of a relaxation process. Their evolutions show that the relaxation times in the liquid increase as T is lowered. (T_ω) is the temperature where the characteristic enthalpy relaxation time of the sample $\tau(T_\omega) = 1/\omega$ is the most probable. The high temperature limit of C' includes the contribution of all activated degrees of freedom of the metastable liquid. The 'static' value of the specific heat is thus recovered. At low temperature, the slowest structural relaxations (so-called α or primary relaxations) are frozen on a time scale shorter than $\tau(T_\omega)$ and only the fastest relaxations and vibrations contribute to the low temperature limit.

From the measurements we can obtain spectroscopic information about the activation energy and the (non) exponentiality of the slow (α) relaxations. The available modulation periods limit the domain of investigation to the temperatures just above T_g which are however that of the metastable liquid in equilibrium.

Non Arrhenius character: fragility index m

Figure 4b shows the relaxation time, on a log scale, vs. inverse peak temperature T_ω^{-1} . Data follow an Arrhenius law

$$\tau = \frac{1}{\omega} = \tau_0 \exp\left(\frac{E}{T_\omega}\right) \quad (10)$$

as expected for the narrow investigated frequency domain. Fitted values of the activation parameters are: activation energy $E \approx 54000$ K, prefactor $\tau_0 \approx 10^{-72}$ s. These values have no direct physical meaning, they however reveal an overall non Arrhenius temperature dependence of the relaxation times. It has been proposed [19, 20] to characterize this non Arrhenius behaviour by a fragility, or stepness index m , defined as

$$m = \frac{d \log_{10} \tau}{d(T_g/T)} \Big|_{T=T_g} = \frac{E}{T_g (\tau=100\text{s}) \ln(10)} \quad (11)$$

E is the apparent activation energy at T_g where T_g is arbitrarily identified with the temperature at which the relaxation time equals 100 s. m is the slope measured at T_g in an Arrhenius plot where the temperature is rescaled to T_g . This definition which allows to compare the degree of non Arrhenius behaviour of different glass formers is directly accessible to MDSC specific heat spectroscopy measurements. For

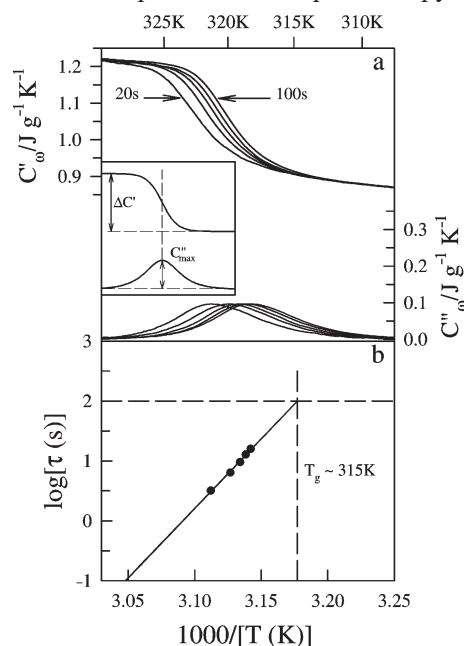


Fig. 4 Real and imaginary parts of the complex specific heat $C_p^*(\omega)$ as a function of reciprocal temperature on cooling ($q = -0.1 \text{ K min}^{-1}$) for indomethacin (a). Enthalpic relaxation times evolution in a log scale as a function of the reciprocal temperature. The full line is the result of a fit with an Arrhenius law (b). Insert: schematic representation of the evolutions in temperature of the real and imaginary part of the complex heat capacity. The position of the maximum in $C_p''(T)$ corresponds to the inflection point in $C_p'(T)$. The $\Delta C'$ and C''_{max} values are used hereafter to determine the stretched exponent β

indomethacin, we find $m=77$ which is a typical value of a fragile glass former ($m\approx 16$ for the strong liquids (SiO_2) and $m>100$ for the most fragile liquids (polymers [19])). This value is in good agreement with the fragility deduced from dynamical mechanical analysis [21, 22].

Non exponential relaxation

The relaxations of the glass formers are usually non exponential and it has been shown that this tendency is more pronounced as the glass former is more fragile [23]. The description of the non exponential character is often made using the fractional exponent β of the Kolhrausch–Williams–Watt (KWW) relaxation function of any investigated quantity:

$$\phi(t)=\exp(-(t/\tau)^\beta) \quad (13)$$

In our case the relaxation which is followed is that of enthalpy. From the fluctuation-dissipation theorem [24] the frequency dependent specific heat $C_p^*(\omega)$ is directly related to the Fourier transform of the time derivative of $\phi(t)$. When operating in the frequency domain, the value of β can be extracted from $C_p^*(\omega)$, β being related to the width of the imaginary part C'' . The present method is operated in the isochronal mode and the shape of the susceptibility $C_\omega^*(T)$ curves not only depends on the stretched exponent β but also on the effective value of the activation energy in the temperature domain of the loss peak. The number of required parameters thus increases uncertainty in a fit procedure. As was proposed by Böhmer *et al.* [25], β can be estimated in a way that is free from an assumption about the temperature-dependence of the relaxation time. In the ideal case of an exponential Debye relaxation function, the magnitude of the loss peak C'' normalized by the dispersion step $\Delta C' = C'_{\omega=0} - C'_{\omega=\infty}$ is 0.5 (insert Fig. 4). $C'_{\text{max}}/\Delta C'$ becomes smaller when β decreases with increasing departures from exponential decay. This correlation has been tabulated by Moynihan *et al.* [26] by evaluation of the Fourier transform of the derivative of the decay (KWW) function and shown to quickly give an accurate value of β . This analysis gives $\beta\approx 0.55$ for indomethacin, close to T_g . This reveals the non exponential character which correlates well with the rather fragile character of the compound [23].

Confrontation of calorimetric and dielectric spectroscopic data

Dielectric spectroscopy is often used to study the dynamical properties of amorphous molecular substances [27]. Its relevance in the investigation of pharmaceutical compounds has been shown in reference [28]. It has been used recently in parallel with the MDSC technique as a mean of characterising the thermal transitions in indomethacin [29]. It is interesting to compare the results of the specific heat and dielectric spectroscopies from the point of view of the shapes of the relaxation functions and the temperature evolution of the peak frequencies. Figure 5 shows confrontation of the isochronal specific heat ($C_{\text{p}\omega}^*(T)$) and dielectric ($\epsilon_\omega^*(T)$) susceptibilities. The general

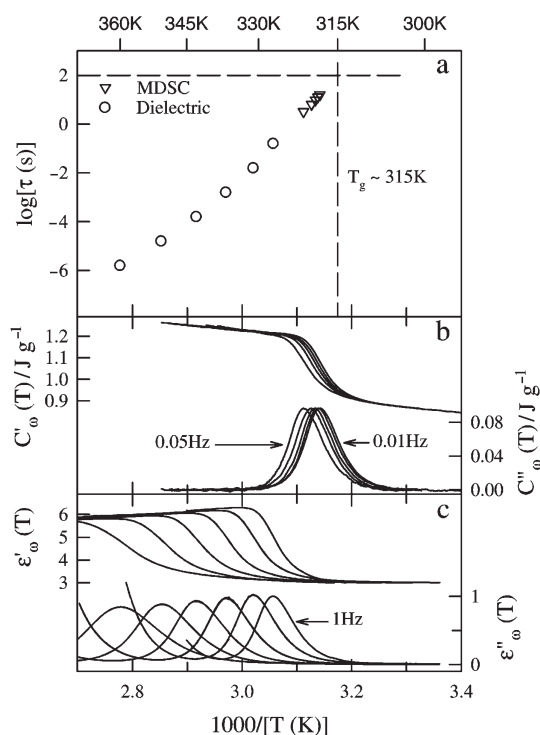


Fig. 5 Confrontation of dielectric (c) and specific heat (b) spectroscopies: the isochronal real $\epsilon'_{\omega}(T)$ and imaginary $\epsilon''_{\omega}(T)$ parts of the dielectric susceptibility of indomethacin are measured on cooling ($q = -0.1 \text{ K min}^{-1}$). The curves, represented as a function of the reciprocal temperature, refer to frequencies 100 KHz–1 Hz in steps of one decade, in the order of decreasing temperature. Dielectric and enthalpic relaxation times are determined from the position of the $\epsilon''_{\omega}(T)$ and $C''_{\omega}(T)$ maxima and are reported in an Arrhenius plot (a)

shapes of the real and imaginary parts of the susceptibilities clearly look quite similar to one another. In addition, there is a perfect continuity in their temperature evolutions. When the frequency decreases, the loss peak $\epsilon''_{\omega}(T)$ narrows and its width at half maximum recovers that of the $C''_{\omega}(T)$ curve. The magnitudes of the normalised peaks height also become identical: $\chi''_{\text{max}}/\Delta\chi' \approx 0.3$. As a consequence, for the same frequency both spectroscopies give identical values of the stretched exponent β . Since dielectric spectroscopy extends the data toward high temperature, it also reveals a very slight increase of β when temperature increases. The dielectric and specific heat relaxation times both determined from the position of the peaks maximum are shown in an Arrhenius plot. This figure shows that the low temperature MDSC data fall into line with the dielectric ones. Furthermore, the tendency of a global non-Arrhenius behaviour foreseen from the unphysical values of the MDSC data refinements is confirmed. In supercooled liquids a Vogel–Fulcher–Tamman (V.F.T.) equation:

$$\tau = \tau_{\text{vf}} \exp\left(\frac{DT_0}{T - T_0}\right) \quad (14)$$

is generally found to give an accurate representation of $\tau(T)$ on a wide frequency range. T_0 is a positive temperature and the dimensionless parameter D is called the strength index [23]. When $T_0=0$, the familiar Arrhenius equation results. The fragility parameter extracted from the V.F.T. refinement gives $m=79$. This value is closed to the value determined from the MDSC measurements by calculating the slope of the relaxation time at T_g . It confirms the coherency between MDSC and dielectric spectroscopies.

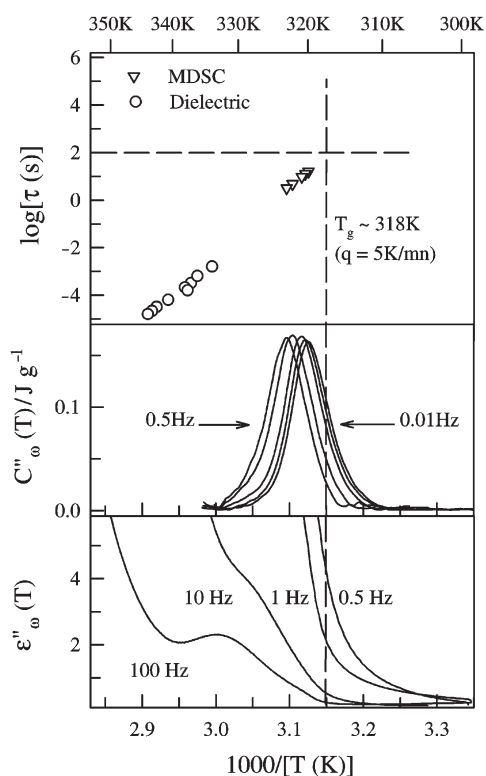


Fig. 6 The imaginary part of the enthalpic $C''_{\omega}(T)$ and dielectric $\epsilon''_{\omega}(T)$ susceptibilities for maltitol at different frequencies. In the frequency domain accessible with MDSC, the dielectric relaxation processes are occulted by the high ionic conductivity contribution of maltitol. The corresponding relaxation times (taken at the maximum of the loss curves) are reported in an Arrhenius plot. Data are taken on cooling at a rate of $q = -0.5 \text{ K min}^{-1}$

Complementarity of MDSC and dielectric measurements: the case of maltitol

Indomethacin is a favorable case to test the validity of MDSC spectroscopy data since dielectric measurements are also available in close frequencies range. This has been used in this paper to demonstrate the coherency of both spectroscopy. There are however frequent situations where dielectric measurements can not be achieved at low frequency due to parasitic conductivity limitations – and also of course when the molecules are non-polar. These are cases where MDSC is likely to provide valuable information about the molecular mobility close to T_g . We illustrate that point on the case of maltitol which is largely used as a dietary food and excipient in pharmaceutical science. MDSC spectra have been published recently [4]. We put these data in parallel (Fig. 6) with dielectric isochronal measurements as was done for indomethacin.

A noticeable feature of the temperature evolution of the loss factor $\epsilon''_{\omega}(T)$ concerns the important high temperature conductivity contribution which makes the primary dielectric α relaxation data of maltitol only accessible within a restricted frequency range. When the frequencies are lower than 10 Hz, the conductivity effects become so large that the relaxational contribution no more appears on the dielectric response. On the other hand, a relaxation peak is perfectly resolved on the $C''_{\omega}(T)$ curves in this frequency domain.

The relaxation times of maltitol deduced from these two techniques are compared in Fig. 6. Whereas the determination of the fragility index m and the stretched exponent β is not possible from the dielectric data alone, the MDSC data allows to obtain $\beta(T_g)=0.42$ and $m=75$. This value of the fragility agrees with that deduced from mechanical measurements [30]. In addition to the complementarity of the two techniques revealed by this figure, we can again observe the coherency of the relaxation times measured. MDSC can be then considered as an excellent substitute technique to the dielectric analysis when dielectric spectroscopy fails to characterise the molecular mobility. This property is particularly useful in all the situations where the electric conductivity is important which is the case of most of hydrated compounds. Generally, these high ionic conductivity systems are also those which present the best thermal conductivity. They give therefore a MDSC signal greatly well resolute.

* * *

This work was supported by a grant from the Interreg II program 'Metastable Molecular Materials' between Nord – Pas de Calais and Kent. We are grateful to the region Nord – Pas de Calais for its help in this program.

References

- 1 B. C. Hancock and G. Zografi, *J. Pharm. Sci.*, 86 (1997) 1.
- 2 B. C. Hancock, S. L. Shamblin and G. Zografi, *Pharm. Res.*, 12 (1995) 799.
- 3 S. L. Shamblin, X. Tang, L. Chang, B. C. Hancock and M. J. Pikal, *J. Phys. Chem.*, 103 (1999) 4113.

- 4 O. Bustin and M. Descamps, *J. Chem. Phys.*, 110 (1999) 1.
- 5 J. M. Hutchinson, *Thermochim. Acta*, 324 (1998) 165.
- 6 J. E. K. Schawe, *Thermochim. Acta*, 260 (1995) 1.
- 7 J. E. K. Schawe, *Thermochim. Acta*, 261 (1995) 183.
- 8 K. J. Jones, I. Kinshott, M. Reading, A. A. Lacey, C. Nikopoulos and H. M. Pollock, *Thermochim. Acta*, 304/305 (1997) 187.
- 9 J. E. K. Schawe and G. W. H. Höhne, *Thermochim. Acta*, 287 (1997) 213.
- 10 B. Wunderlich, Y. Jin and A. Boller, *Thermochim. Acta*, 238 (1994) 277.
- 11 J. E. K. Schawe and W. Winter, *Thermochim. Acta*, 298 (1997) 9.
- 12 Z. Jiang, C. T. Imrie and J. M. Hutchinson, *Thermochim. Acta*, 315 (1998) 1.
- 13 S. Weyer, A. Hensel and C. Schick, *Thermochim. Acta*, 304/305 (1997) 267.
- 14 L. Carpentier, O. Bustin and M. Descamps, *J. Phys. D: Appl. Phys.*, 35 (2002) 402.
- 15 N. O. Birge and S. R. Nagel, *Phys. Rev. Lett.*, 54 (1985) 2674.
N. O. Birge, *Phys. Rev. B*, 34 (1986) 1631.
- 16 M. Yoshioka, B. C. Hancock and G. Zografi, *J. Pharm. Sci.*, 83 (1994) 1700.
- 17 E. Fukuoka, M. Makita and S. Yamamura, *Chem. Pharm. Bull.*, 34 (1986) 4314.
- 18 M. Siniti, Etude thermodynamique des phénomènes de relaxation des matériaux vitreux. Caractérisation de l'état enthalpique d'un verre de polyol dans le domaine de la transition vitreuse, Ph. D. Thésis, Institut National des Sciences Appliquées de Lyon, 1995.
- 19 R. Böhmer, K. L. Ngai, C. A. Angell and D. J. Plazcek, *J. Chem. Phys.*, 99 (1993) 4201.
- 20 C. A. Angell, *J. of Res. of the National Institute of Standards and Technology*, 102 (1997) 171.
- 21 V. Andronis and G. Zografi, *Pharm. Res.*, 14 (1997) 410.
- 22 V. Andronis and G. Zografi, *Pharm. Res.*, 15 (1998) 835.
- 23 R. Böhmer and C. A. Angell, Local and global relaxations in glass forming materials, in *Disordered effects on relaxational processes*, Springer-Verlag, Eds R. Richert and A. Blumen, 1994.
- 24 J. K. Nielsen and J. C. Dyre, *Phys. Rev. B*, 54 (1996) 15754.
- 25 R. Böhmer, E. Sanchez and C. A. Angell, *J. Phys. Chem. B*, 96 (1992) 9089.
- 26 C. T. Moynihan, L. P. Boesch and N. L. Laberge, *Phys. and Chem. of Glasses*, 14 (1973) 122.
- 27 F. Z. Stickel, *Untersuchung der dynamik in niedermolekularen flüssigkeiten mit dielektrischer spektroskopie*, Verlag Shaker, Aachen 1995.
- 28 D. Q. M. Craig, *Dielectric analysis of pharmaceutical systems*, Taylor & Francis, 1995.
- 29 R. He and D. Q. M. Graig, *J. Pharm. Pharmacol.*, 53 (2001) 41.
- 30 A. Faivre, L. David and J. Perez, *J. Phys. II France*, 11 (1997) 1635.